OPTOELECTRONICS AND ADVANCED MATERIALS – RAPID COMMUNICATIONS Vol. 1, No. 9, September 2007, p. 467 - 470

Optimization of alloy composition, interlayer and barrier thicknesses in $Al_xGa_{1-x}N$/(AlN)/GaN high electron mobility transistors

S. B. LISESIVDIN*, A. YILDIZ[a], M. KASAP
Gazi University, Faculty of Science and Arts, Physics Department, Teknikokullar, Ankara, Turkey
[a]Ahi Evran University, Faculty of Science and Arts, Physics Department, Kirsehir, Turkey

The investigating of the GaN-based high electron mobility transistors (HEMTs) is focused to achieve two goals: increase of carrier density and mobility. Increasing the number of the carriers in the 2-dimensional-electron-gas (2DEG) and localize the carriers in the 2DEG properly are required to achieve high performance. Inserting a thin undoped AlN interlayer between undoped $Al_xGa_{1-x}N$ barrier and undoped GaN channel layer is one of the methods to achieve high performance $Al_xGa_{1-x}N$/GaN HEMT structures. In this work, self-consistent 1-band 1-dimension Schrödinger-Poisson equations are solved for pseudomorphically grown undoped $Al_xGa_{1-x}N$/GaN HEMT structures with and without AlN interlayer. The effects of AlN interlayer and $Al_xGa_{1-x}N$ barrier layer thicknesses and different Al-mole fractions in $Al_xGa_{1-x}N$ barrier layer on band structures, carrier densities and 2DEG wave functions are investigated.

(Received August 6, 2007; accepted August 30, 2007)

Keywords: AlGaN/GaN, HEMT, Schrödinger equation, Poisson equation, 2DEG, AlN interlayer, AlGaN barrier

1. Introduction

Rectifiers and high power switches for electricity networks, microwave integrated circuits, modulators and power amplifiers for new generation wireless communication stations and other many applications require more performances than Si-based or GaAs-based devices can provide. $Al_xGa_{1-x}N$/GaN HEMTs are showed their capacity for high power and high frequency applications [1]. Unlike Si and GaAs, GaN-based HEMT structures have strong spontaneous and piezoelectric polarization, which causes 2DEG with high sheet carrier density values, without intentional doping. In order to improve the performance of $Al_xGa_{1-x}N$/GaN HEMTs, it is necessary to increase both carrier density and mobility of the 2DEG. For increasing 2DEG carrier density, modulation doping at AlGaN barrier can be done, but this increase is limited with doping [2, 3]. Another successful method to increase 2DEG carrier density is raising Al mole fraction of AlGaN barrier. This will provide more spontaneous and piezoelectric polarization fields, which will induce higher 2DEG carrier densities, but with increasing mole fraction, mobility will drop due to alloy disorder scattering. Another important approach to achieve high performance is inserting an AlN interlayer between $Al_xGa_{1-x}N$ barrier and GaN layer which is studied recently by several groups [4-8].

Design and fabrication of such devices requires more rapid and accurate simulation analyses to perform successful electronic and optical optimizations. Due to exponential increase in the computing power and fast decrease in costs of computer hardware and software, computational physics is now more convenient tool for optimization of semiconductor devices, especially wurtzite GaN-based devices which have quantum confinement regions, strain induced polarization fields and polarization induced carriers. A number of groups have investigated different methods to solve Poisson's and Schrödinger's equation [9, 10]. We prefer to solve self-consistent non-linear Schrödinger-Poisson equation because of its accuracy.

In this work, we model $Al_xGa_{1-x}N$/GaN and $Al_xGa_{1-x}N$/(AlN)/GaN HEMT structures with solving self-consistent non-linear Schrödinger-Poisson equation [11]. The effects of AlN interlayer and $Al_xGa_{1-x}N$ barrier layer thicknesses and different Al-mole fractions in $Al_xGa_{1-x}N$ barrier layer on band structures, carrier densities and 2DEG wave functions are investigated.

2. Simulation

Inserting an AlN interlayer between $Al_xGa_{1-x}N$ barrier and GaN layer will make polarization effects stronger and this causes a higher sheet carrier density, and due to less alloy disorder scattering, a higher mobility can be achieved [4-8]. We simulate $Al_xGa_{1-x}N$/GaN HEMT structures with and without AlN interlayer for different $Al_xGa_{1-x}N$ barrier layer alloy compositions (x) and different AlN interlayer thicknesses. Simulation procedure begins with strain calculation with homogeneous strain dispersion over the simulated region. Strain in a GaN-based material produces a large piezoelectric polarization which affects directly the electronic and optical properties of material. With calculated strain and the pyroelectric charges, piezoelectric charges are calculated. Taking piezoelectric charges into account is important, because nearly all carriers are caused by this piezoelectricity in unintentionally doped GaN-based semiconductors. After the calculation of the piezoelectric charges, these piezoelectric and pyroelectric charges are used to solve

Poisson equation. In the last step of the simulation, Schrödinger's equation and the Poisson's equation are solved self-consistently to obtain the carrier distribution, wave functions and related eigenenergies. The material parameters of AlN and GaN which are used by the simulator are taken from several references [12-15], and the $Al_xGa_{1-x}N$ parameters are deduced using Vegard's law.

Conduction band structures, electron densities and wave functions of the electrons are found for different AlN interlayer thicknesses, $Al_xGa_{1-x}N$ barrier layer thicknesses and Al mole fraction in AlGaN barrier including piezoelectric effects. In the calculation of the probability densities of the electrons program has been used one-band effective mass model which is a reliable model [16, 17].

3. Results and discussion

Conduction band structures of $Al_xGa_{1-x}N/GaN$ HEMT structures with and without AlN interlayer are shown in Fig. 1. Both simulated structures have a 3 nm GaN cap layer which provides enhancement of the effective Schottky barrier and provides smaller gate leakages and causes reduction in sheet carrier density in the channel [18, 19]. GaN cap layer is thin to form 2DEG at the $GaN/Al_xGa_{1-x}N$ interface. The addition of the AlN interlayer increases the conduction band offset ΔE_c in the $Al_xGa_{1-x}N$ barrier layer. Thicknesses of the simulated AlN interlayers are in the limit of the strain relaxation mechanism [20]. The 2DEG formation at the AlN/GaN interface is deeper than the $Al_xGa_{1-x}N/GaN$ interface which will supply better localization of the electrons in the well [21].

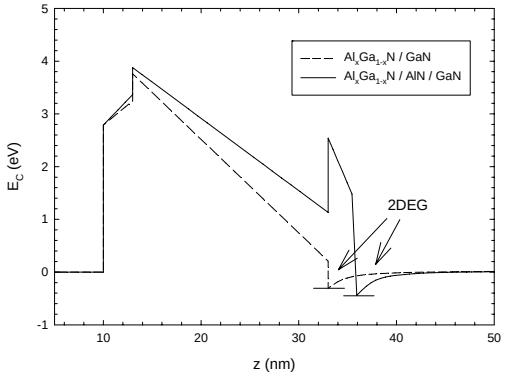

Fig. 1. The band structure of $Al_xGa_{1-x}N/GaN$ and of $Al_xGa_{1-x}N/(AlN)/GaN$ structures for x = 0.35, Z-axis begins from the surface.

Future investigations of the $Al_xGa_{1-x}N/(AlN)/GaN$ HEMT systems depend on the structure designs as well as material quality. To increase 2DEG conductivity and breakdown field, higher Al-mole fraction at barrier layer is required [22]. However, the growth process of high-Al mole fraction layers on GaN is a problematic due to large lattice parameter mismatch which can cause defects due to strain relaxation [23]. Because the transport properties of the 2DEG of the HEMT structures are limited by the strain relaxation, the number of reports about transport properties of the HEMT structures with a barrier layer having an Al-mole fraction of x > 0.5 is also limited [24, 25]. In our calculations, two structural designs were investigated: inserting an AlN interlayer between $Al_xGa_{1-x}N$-GaN interface and increasing the mole fraction of the $Al_xGa_{1-x}N$ barrier. In Fig. 2 (a), effect of the AlN interlayer thickness on sheet carrier density is shown for the structure with $Al_{0.35}Ga_{0.65}N$ barrier. Sheet carrier density is increasing with increasing AlN interlayer thickness. Due to large lattice mismatch between GaN and AlN layer, investigation of pseudomorphic growth of AlN layer on GaN above 5 nm is senseless [26, 27]. With increasing interlayer thickness, sheet carrier density approaches to 2 x 10^{11} cm^{-2}. In Fig. 2 (b), Sheet carrier density due to $Al_xGa_{1-x}N$ barrier thickness is shown for x=0.25, 0.35 and 0.45. Sheet carrier density is increasing with increasing $Al_xGa_{1-x}N$ barrier thickness. It is important to investigate the values consistent with AlN thickness. More Al-fraction, increases sheet carrier density, but increases alloy disorder scattering, too. To prevent this, thicker AlN is needed, but it is hard to grow thicker AlN on GaN without strain relaxation. Under these circumstances, alloy fraction of x=0.35 can be accepted for the most available applications.

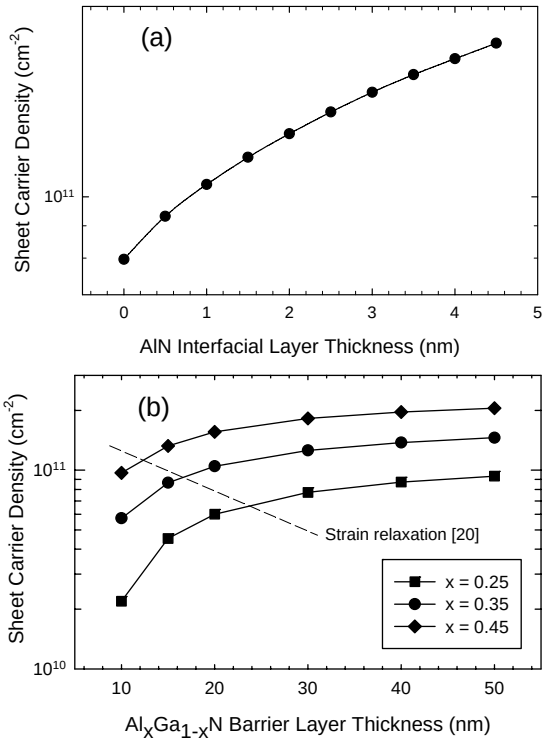

Fig. 2. (a) Sheet carrier density versus AlN interlayer thickness for a structure with a $Al_{0.35}Ga_{0.65}N$ barrier layer. (b) Sheet carrier density versus $Al_xGa_{1-x}N$ barrier layer thickness for x=0.25, 0.35 and 0.45. Strain relaxation according to Bykhovski et al. [20] is also shown.

In Fig. 3, probability density of an electron in well is showed for different structures with different AlN

interlayer thicknesses for the structure with an $Al_{0.35}Ga_{0.65}N$ barrier. Without an AlN interlayer, there is more probable to find an electron in $Al_xGa_{1-x}N$ layer. The electron in $Al_xGa_{1-x}N$ layer is more influenced by alloy-disorder scattering [28]. With a 1 nm and 2 nm thick AlN layer, the electron is more localized in channel. In 2 nm case, probability is nearer to interface. In real structures, this may cause decrease in mobility due to interface roughness scattering, dislocation scattering and alloy-disorder scattering. So, thicker interlayer means more influence on interface related scattering mechanisms. According to Fig. 3, there is no considerable difference of the probability densities between 1nm and 2 nm situations, and according to the results of Hsu et al. [29] electron penetration into AlN is only 0.3 nm which is in good agreement with our result. Here we can state that, 1 nm AlN interlayer is the most logical choice for the most applications available.

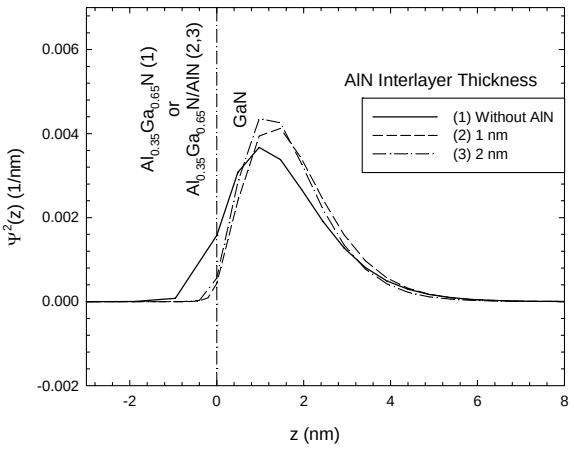

Fig. 3. Probability density of an electron versus normalized distance for different AlN interlayers for the structure with an $Al_{0.35}Ga_{0.65}N$ barrier. Origin of z-axis is located at the interface at which 2DEG is formed ($Al_{0.35}Ga_{0.65}N$/GaN interface for the structure without an AlN interlayer and AlN/GaN interface for the other structures).

In Fig. 4, probability density of an electron in a pseudotriangular well is showed for different structures with different $Al_{0.35}Ga_{0.65}N$ barrier thicknesses. Thicker barrier causes more localized electrons near to AlN/GaN interface. For the same configurations at Fig. 4, depths of the 95% probability of electron from AlN/GaN interface are listed in Table 1. According to Table 1, it is more probable to find an electron far away from AlN/GaN interface for a 5 nm $Al_xGa_{1-x}N$ barrier situation. Like AlN, nearer electron to interface, is more influenced by interface related scattering mechanisms like to interface roughness scattering, dislocation scattering and alloy disorder scattering. But unlike AlN, thinner barrier layer increases the electron probability in the GaN layer which can be effected more from impurity scatterings [30]. So, it can be accepted that 15 nm $Al_{0.35}Ga_{0.65}N$ barrier layer which is below strain relaxation according to Bykhovski et al. [20] (see Fig. 2 (b)) and less affected from both surface and bulk related scatterings, as a most logical choice for the most applications available.

Table 1. Depth of the %95 of a total probability of a electron from AlN/GaN interface versus $Al_{0.35}Ga_{0.65}N$ barrier thicknesses. Values written in italics are above the threshold of strain relaxation [20].

$Al_{0.35}Ga_{0.65}N$ Barrier Thickness (nm)	Depth of 95% of an Electron from AlN/GaN Interface (nm)
5	10.4716
10	4.4374
15	3.8137
20	3.4879
30	3.2330
40	3.1172
50	2.9997

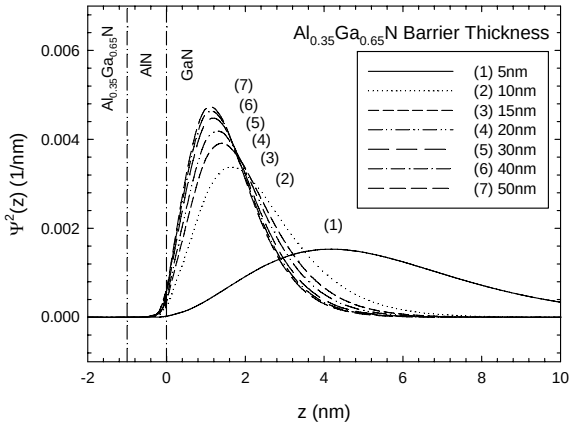

Fig. 4. Probability density of an electron versus normalized distance for the structures with different $Al_{0.35}Ga_{0.65}N$ barrier thicknesses. Origin of z-axis is located at the interface at which 2DEG is formed (AlGaN/GaN interface for the structure without an AlN interlayer and AlN/GaN interface for the other structures).

4. Conclusions

We have modeled $Al_xGa_{1-x}N$/GaN and $Al_xGa_{1-x}N$/(AlN)/GaN HEMT structures with solving self-consistent non-linear Schrödinger-Poisson equations. Band structures, sheet carrier densities and wave functions are found for different AlN interlayer thicknesses, $Al_xGa_{1-x}N$ barrier layer thicknesses and Al-mole fraction of $Al_xGa_{1-x}N$ barrier including piezoelectric effects. Effects of the AlN interlayer, AlGaN barrier layer and Al mole fraction of barrier layer were investigated. For the high performance devices with a high mobility and high carrier density, optimization results for $Al_xGa_{1-x}N$ barrier layer

Al-mole fraction value, AlN interlayer thickness and $Al_xGa_{1-x}N$ barrier thickness are stated for the most applications available. Simulation results and optimization values are in good agreement with the previously reported ones.

Acknowledgements

This work is supported by the State of Planning Organization of Turkey under Grant No. 2001K120590.

References

[1] U. K. Mishra, P. Parikh, Y. –F. Wu, Proc. IEEE **90**, 1022 (2002).
[2] Z. H. Feng, Y. G. Zhou, S. J. Cai, K. M. Lau, Appl. Phys. Lett. **85**, 5248 (2004).
[3] H. Xing, S. Keller, Y. –F. Wu, L. McCarthy, I. P. Smorchkova, D. Buttari, R. Coffie, D. S. Green, G. Parish, S. Heikman, L. Shen, N. Zhang, J. J. Xu, B. P. Keller, S. P. DenBaars, U. K. Mishra, J. Phys.: Condens. Matter **13**, 7139 (2001).
[4] L. Shen, S. Heikman, B. Moran, R. Coffie, N. –Q. Zhang, D. Buttari, I. P. Smorchkova, S. Keller, S. P. DenBaars, U. K. Mishra, IEEE Electr. Device L. **22**, 457 (2001).
[5] R. S. Balmer, K. P. Hilton, K. J. Nash, M. J. Uren, D. J. Wallis, A. Wells, M. Missous, T. Martin, Phys. Stat. Sol. (c) **0**, 2331 (2003).
[6] I. P. Smorchkova, S. Keller, S. Heikman C. R. Elsass, B. Heying, P. Fini, J. S. Speck, U. K. Mishra, Appl. Phys. Lett. **77**, 3998 (2000).
[7] Y. –F. Wu, A. Saxler, M. Moore, R. P. Smith, S. Sheppard, P. M. Chavarkar, T. Wisleder, U. K. Mishra, P. Parikh, IEEE Electr. Device L. **25**, 117 (2004).
[8] I. P. Smorchkova, L. Chen, T. Mates, L. Shen, S. Heikman, B. Moran, S. Keller, S. P. DenBaars, J. S. Speck, U. K. Mishra, J. Appl. Phys. **90**, 5196 (2001).
[9] K. Yokoyama, K. Hess, Phys. Rev. B **63**, 938 (1986).
[10] A. M. Cruz Serra, H. Abreu Santos J. Appl. Phys. **70**, 2734 (1993).
[11] S. Birner, S. Hackenbuchner, M. Sabathil et al., Acta Phys. Pol. A **110**, 111 (2006).
[12] I. Vurgaftman, J. R. Meyer, L. R. Ram-Mohan, J. Appl. Phys. **89**, 5815 (2001).
[13] I. Vurgaftman, J. R. Meyer, J. Appl. Phys. **96**, 3675 (2003).
[14] O. Ambacher, J. Majewski, C. Miskys, A. Link, M. Hermann, M. Eickhoff, M. Stutzmann, F. Bernardini, V. Fiorentini, V. Tilak, B. Schaff, L. F. Eastman, J. Phys.: Condens. Matter **14**, 3399 (2002).
[15] H. Morkoç, "Nitride Semiconductors and Devices" Springer-Verlag, Berlin - Heidelberg (1999).
[16] S. Tomic, E. P. O'Reilly, P. J. Klar, H. Grüning, W. Heimbrodt, W. M. Chen, I. A. Buyanova, Phys. Rev. B **69**, 245305 (2004).
[17] E. P. O'Reilly, A. Lindsay, S. Tomic, P. J. Klar, Phys. Stat. Sol. (b) **241**, 3099 (2004).
[18] B. Jogai, J. Appl. Phys. **93**, 1631 (2003).
[19] S. Heikman, S. Keller, Y. –F. Wu, J. S. Speck, S. P. DenBaars, U. K. Mishra, J. Appl. Phys. **93**, 10114 (2003).
[20] A. Bykhovski, B. Gelmont, M. Shur, J. Appl. Phys. **81**, 6332 (1997).
[21] C. Wang, X. Wang, G. Hu, J. Wang, J. Li, Z. Wang, Appl. Surf. Sci. **253**, 762 (2006).
[22] Y. –F. Wu, D. Kapolnek, J. P. Ibbetson, P. Parikh, B. P. Keller, U. K. Mishra, IEEE T. Electron. Dev. **48**, 586 (2001).
[23] B. Shen, T. Someya, Y. Arakawa, Appl. Phys. Lett. **76**, 2746 (2000).
[24] F. Nakamura, S. Hashimoto, M. Hara, S. Imanaga, M. Ikeda, H. Kawai, J. Cryst. Growth **195**, 280 (1998).
[25] E. Alekseev, A. Eisenbach, D. Pavlidis, Electron. Lett. **35**, 2145 (1999).
[26] G. Feuillet, B. Daudin, F. Widmann et al., J. Cryst. Growth **189/190**, 142 (1998).
[27] N. Grandjean, J. Massies, Appl. Phys. Lett. **71**, 1816 (1997).
[28] M. J. Kearney, A. I. Horrell, Semicond. Sci. Technol. **13**, 174 (1998).
[29] L. Hsu, W. Walukiewicz, J. Appl. Phys. **89**, 1783 (2001).
[30] S. Gökden, Phys. Stat. Sol. (a) **200**, 369 (2003).

*Corresponding author: sblisesivdin@gmail.com